Effect of Agitation on Crystallization Behavior of $CaO-Al_2O_3-SiO_2-Na_2O-CaF_2$ Mold Fluxes with Varying Basicity

JIANGLING LI, QIFENG SHU, and KUOCHIH CHOU

The effect of agitation on crystallization behaviors of $CaO-Al_2O_3-SiO_2-Na_2O-CaF_2$ mold fluxes with basicity of 1.1 and 1.2 was investigated. It was found that crystallization temperatures of agitated samples were higher than those of static samples. The morphology of cuspidine shifted from dendrites to facet crystals with the decrease of temperature. The agitation was conducive to the formation of small dendritic cuspidine and could lead to crystals with smaller size. Crystalline fraction could be significantly enhanced by agitation at the initial stage of crystallization.

DOI: 10.1007/s11663-015-0357-3

I. INTRODUCTION

MOLD fluxes play an indispensable role in the continuous casting process of steel. It is due to the fact that mold flux could provide the following functions[1–4]: (1) protecting the meniscus of the steel from oxidation; (2) providing thermal insulation; (3) providing liquid fluxes to lubricate the strand; (4) provide the optimal level of heat transfer; and (5) absorbing inclusions from the steel. These functions are closely related to the quality of casting products. It is well known that the viscosity and crystallization behaviors of mold fluxes are two of the most important parameters to ensure implementations of above-mentioned functions.[2,5,6] Suitable viscosity and crystallization behavior of mold fluxes can ensure the full lubrication and effective heat transfer control in the casting of steel.

During the casting process, the oscillation of copper mold will generate shear stress on mold fluxes, which could cause variation on the property of mold fluxes, *e.g.,* crystallization behavior.[7,8] As a result, there could emerge casting problems if effects of the external force field on mold fluxes are not well understood. In order to accurately evaluate the performance of mold fluxes, it is essential to study the effects of shear stress field on the mold flux.

There are only a few studies dealing with effects of shear stress fields on the crystallization of slags.[9–11] Saito *et al.*[10] firstly exerted a shear stress field to slag by agitating the liquid slag using a Pt-Rh rod, and investigated the effects of agitation on crystallization behavior of $CaO-SiO_2-R_2O$ (R = Li, Na, or K). The crystallization temperature was determined using a novel technique which is based on the difference in electrical permittivity of the ionic liquid and solid. They found that crystallization temperatures of investigated slags were increased by agitation. Harada *et al.*[11] employed the similar method to investigate the effect of agitation on crystallization behavior of $CaO-SiO_2-CaF_2$ melts. The results showed that crystallization of dendritic $CaO{\cdot}SiO_2$ was strongly affected by the agitation and the crystallization of faceted cuspidine ($Ca_4Si_2O_7F_2$) showed little dependence on the agitation. However, it can be seen that previous studies are mainly about the simple slag systems, and there is no reference about the multicomponent slag systems.

In the present work, the effects of agitation on crystallization of the multicomponent mold flux systems with varying basicity (defined as R = w(CaO)/w(SiO_2), w(CaO), and w(SiO_2) are mass percentages of CaO and SiO_2) were investigated by agitating the mold fluxes with rotations of molybdenum rod. In view of the fact that cuspidine is the dominant crystal for the traditional mold flux to control the heat transfer,[6] this study focused on the effects of agitation field on the morphology and size of cuspidine in mold fluxes.

II. EXPERIMENTAL

A. *Material Preparation*

Reagent grade powders of $CaCO_3$ (>99.5 mass pct), SiO_2 (>99.5 mass pct), Al_2O_3 (>99.5 mass pct), Na_2CO_3 (>99.5 mass pct), and CaF_2 (>99 mass pct) were used as raw materials. $CaCO_3$ was calcined in a muffle furnace for 10 hours at 1323 K (1050 °C) to obtain CaO. Na_2CO_3, SiO_2, CaF_2, and Al_2O_3 powders were also calcined at 873 K (600 °C) to remove moisture. Designed compositions of fluxes used in the present study are given in Table I.

JIANGLING LI, Doctoral Student, QIFENG SHU, Associate Professor, and KUOCHIH CHOU, Professor, are with the State Key Laboratory of Advanced Metallurgy, University of Science and Technology, Beijing 100083, P.R. China, and also with School of Metallurgical and Ecological Engineering, University of Science and Technology, Beijing 100083, P.R. China. Contact e-mail: shuqifeng@gmail.com

Manuscript submitted January 11, 2015.
Article published online April 28, 2015.

Table I. Designed Chemical Composition of the Studied Mold Fluxes

Sample No.	Composition (mass pct)					
	CaO	Al_2O_3	SiO_2	CaF_2	Na_2O	CaO/SiO_2
1	37.7	5	34.3	15	8	1.1
2	39.3	5	32.7	15	8	1.2

B. *Experimental Procedure*

The schematic diagram of the experimental apparatus is shown in Figure 1. The molybdenum rod was directly applied to agitate the fluxes. After melting of flux, Mo rod was immersed into the molten flux for 30 mm and rotated with a speed of 100 r/min. At the end of the experiment, the molybdenum rod was removed from the furnace and cooled. The experiments were conducted in a molybdenum silicide vertical tube furnace under argon atmosphere. Temperature inside furnace was measured using a Pt-6 pct Rh/Pt-30 pct Rh (B type) thermocouple placed underneath the bottom of crucible. A graphite crucible with 55-mm inner diameter and 100-mm depth was used to melt the flux. After accurately weighed with an appropriate mass proportion, the 160 g powder mixture was ground thoroughly in a mortar and melted in a graphite crucible in a molybdenum silicide vertical tube furnace under argon atmosphere for 2 hours at 1623 K (1350 °C). Then, the furnace temperature was cooled to a target temperature at the rate of 5 K/min. After reaching each target temperature, the melt was maintained at the temperature for 15 minutes. Isothermal stage for 15 minutes was arranged in order to ensure the temperature equilibrium. Long-time isothermal stage was not applied due to the fact it would lead to thermodynamic phase equilibrium and eliminate the difference between static samples and agitated sample. Subsequently, parts of fluxes were extracted by quartz glass tube and quenched by water to analyze the crystallization behaviors. The extractions of fluxes were carried out at every 20 K (20 °C) interval on cooling, and afterward the melts were cooled to the next target temperature at the rate of 5 K/min. Experiments for crystallization of fluxes at static condition (with no revolution of rod) were performed for comparison in all samples. The cooling regime for experiments performed at static condition was as same as that for experiments with agitation. The quenched sample extracted from mold fluxes with no agitation by Mo rod was denoted by ''static samples,'' while quenched samples from mold fluxes under agitation were denoted by ''agitated samples'' in the present work.

Samples extracted at target temperatures were analyzed by scanning electronic microscopy equipped with energy-dispersed spectroscopy (SEM–EDS) and powder X-ray diffraction (XRD) to identify the crystalline phase and investigate crystalline morphology. Samples were mounted with resin, and then ground and polished for SEM–EDS analysis. SEM–EDS analysis was performed on a scanning electronic microscopy (FEI-MLA250) equipped with a Bruker energy-dispersed spectroscopy. The working voltage is 25 kV. XRD measurements were carried out in air on an X-ray diffractometer (M21X-SRA, MAC Science) equipped with graphite crystal monochromator.

Differential thermal analyses (DTA) were carried out to determine the crystallization temperatures of the investigated mold fluxes. DTA was performed in argon atmosphere on each of the glassy powder samples at the range from 373 K to 1623 K (100 °C to 1350 °C) using a TG–DTA calorimeter (STA 449C, Netzsch) at the cooling rate of 5 K/min. α-alumina was used as a reference material. For each DTA measurement, approximate 20 mg powder sample was used.

The chemical compositions of agitated samples cooled to ambient temperature were determined by using X-ray fluorescence analysis (XRF) (Shimadzu XRF 1800) and are listed in Table II. The carbon contents in agitated samples cooled to ambient temperature were determined using a carbon/sulfur analyzer (Horiba, EMIA-820V) and also listed in Table II. XRD analysis was employed to determine the phase compositions of agitated samples cooled to ambient temperature.

III. RESULTS AND DISCUSSION

Results of DTA measurements are shown in Figure 2. It could be seen from the figure that there was only one exothermic peak on each DTA curve, indicating the presence of one crystallization event for each sample. The crystallization temperature for one phase corresponds to the temperature at which the crystallization just begins in the non-isothermal crystallization process and can be determined as the onset temperature of an exothermic peak during cooling. Crystallization temperature for the first crystalline phase precipitated in mold flux is designated to be the crystallization temperature of mold flux.[12] It can be obtained from DTA curves that the crystallization temperature increased from 1504 K to 1524 K (1231 °C to 1251 °C) with increasing basicity of samples. The increase of crystallization temperature with increasing basicity indicated that increasing basicity promoted the crystallization of mold fluxes, which has been found by many researchers.[13–15] With the increase of basicity, silicate network was depolymerised, leading to decrease of viscosity of mold fluxes. The energy barrier for ions transfer from to melts to melt-crystal interface was lowered and the activation energy required for crystal growth was reduced. Accordingly, the crystallization of mold fluxes was promoted.

Figure 3 compares XRD patterns of agitated samples with those of static samples quenched from high

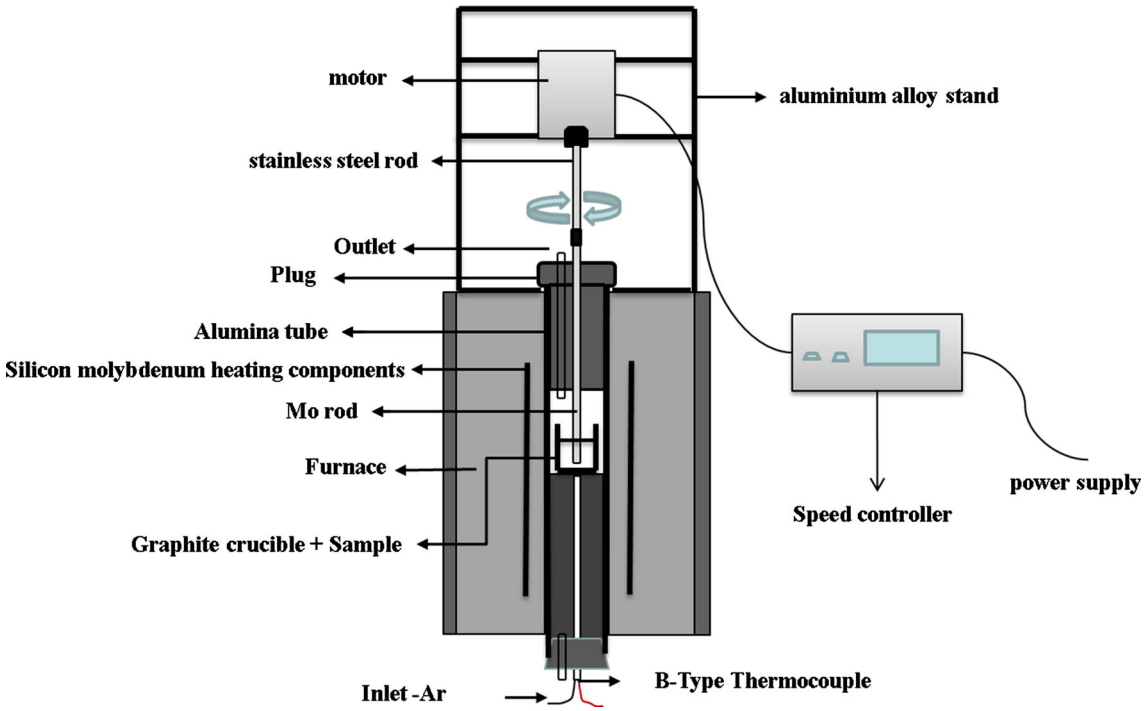

Fig. 1—Schematic diagram of experimental apparatus.

Table II. Analyzed Chemical Composition of the Studied Mold Fluxes After Crystallization Under Agitation

	Composition (mass pct)						
Sample No.	CaO	Al_2O_3	SiO_2	CaF_2	Na_2O	MoO_3	C
1	41.52	3.10	34.76	13.96	6.56	0.09	0.062
2	42.00	3.05	33.80	15.14	4.86	1.14	0.070

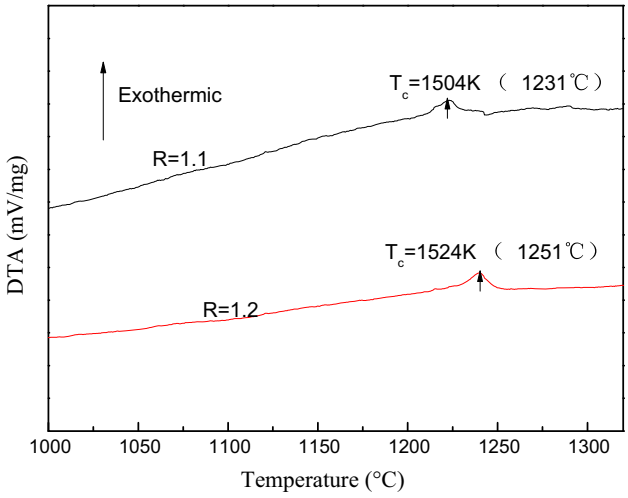

Fig. 2—Results of DTA measurements for the investigated mold fluxes.

temperature. Diffraction peaks of cuspidine could be found in the agitated sample with $R = 1.1$ and the static sample with $R = 1.2$, and no diffraction peaks of other crystal could be found in all samples. Figure 4 shows the XRD patterns of the agitated samples which were cooled to the ambient temperature. It could be found that there are only diffraction peaks of cuspidine in the patterns, which indicate that cuspidine is the only crystalline phase precipitated from mold fluxes investigated. Since the same cooling rate was applied in non-isothermal heat treatment as that in DTA measurements, it could be inferred from the XRD results that the single exothermic peak for mold fluxes with the basicities of $R = 1.1$ and 1.2 corresponds to the formation of cuspidine. Seo *et al.*[14] investigated the effect of basicity on crystallization of liquid mold fluxes using differential scanning calorimetry (DSC), and found that only cuspidine crystallized in the mold fluxes with a high basicity. According to a phase equilibrium study on $CaO\text{-}CaF_2\text{-}SiO_2\text{-}Al_2O_3$ flux system,[16] cuspidine was firstly precipitated as the primary crystal for flux with a basicity higher than $R = 1$ ($Al_2O_3 = 9$ pct). The present investigation is consistent with these previous reports.

There was no diffraction peak found in the XRD pattern of static sample with $R = 1.1$ and from 1543 K (1270 °C) in Figure 3(a). In comparison, diffraction peaks of cuspidine with the amorphous backgrounds could be found in XRD patterns of agitated sample with

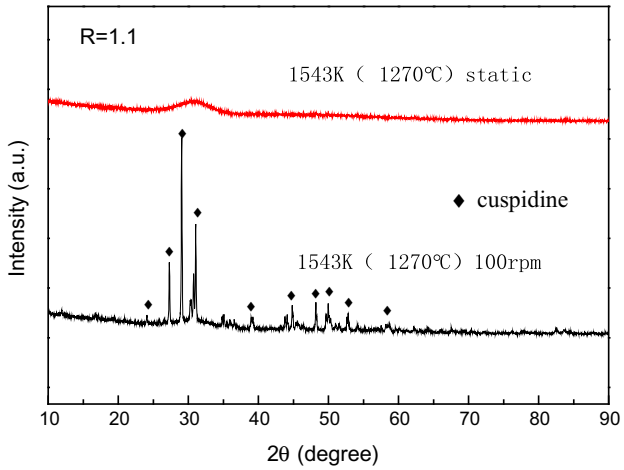

(a) R=1.1

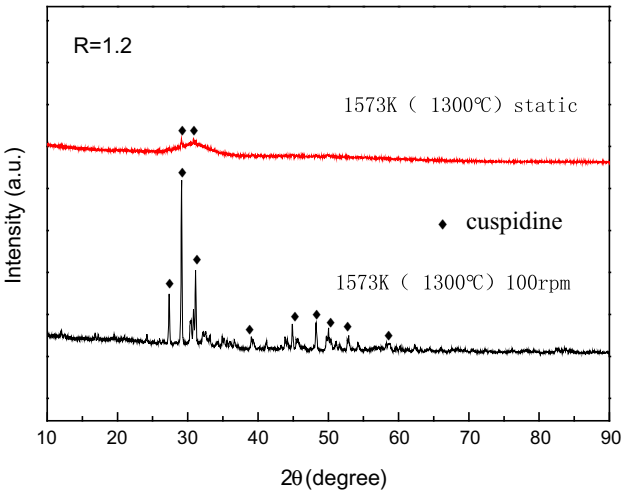

(b) R=1.2

Fig. 3—Comparison between XRD patterns of the agitated samples and those of static samples quenched from high temperature.

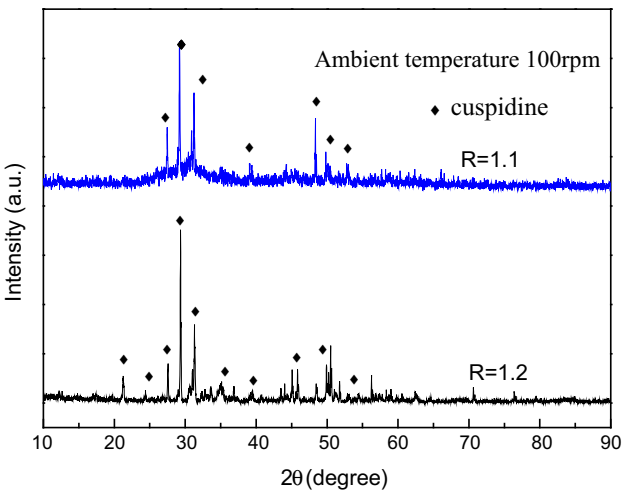

Fig. 4—XRD patterns of the agitated samples cooled to the ambient temperature.

R = 1.1. Meanwhile, there were only several weak diffraction peaks accompanied by strong amorphous backgrounds in the XRD pattern of the static sample with R = 1.2 from 1573 K (1300 °C) in Figure 3(b), while there presented strong diffraction peaks of cuspidine in XRD patterns of the agitated sample. It indicated that cuspidine crystals could form at a higher temperature in agitate mold fluxes and the crystallization temperature was increased by the agitation. This result is consistent to previous reports by Saito *et al.*[10] and Harada *et al.*[11] Forced convection of molten flux induced by agitation accelerated the mass transfer across the crystal-melts interface and promoted to product more nuclei. Therefore, heterogeneous nucleation and growth of crystal were promoted.[17]

Figure 5 shows SEM micrographs of samples of R = 1.1 quenched from different temperatures. The EDS showed that the crystallization product was cuspidine in all samples, which was consistent with the results of XRD. It could be seen from Figure 5(a) that there precipitated many dendrites in the agitated sample at 1543 K (1270 °C). As quenching temperature decreased, there appeared many faceted crystals in samples. Orrling *et al.*[18,19] systematically investigated the crystallization of various slags using Double Hot Thermocouple Technique (DHTT) and found that crystal morphology in experiments was dependent upon the experimental temperature. They classified four different morphologies of crystals based on melt undercooling. At high temperature, they observed many equiaxed crystals which were composed of many dendrites, while many faceted or columnar crystals were observed at lower temperature. Later, similar results were reported by many researchers.[20,21] The present investigation on morphology dependence on temperature is consistent with these previous reports. The dendrites formed at high temperature could be attributed to heterogeneous nucleation followed by crystal growth controlled by heat and chemical diffusion.[19,20] The faceted crystals observed at lower temperature could be precipitated by homogenous nucleation due to larger undercooling.[20] The faceted morphology indicates that the crystal growth is controlled by reaction at crystal-melt interface.[22]

As could be seen from Figure 5(a), there were some cloudy like light gray phases in micrograph of the static sample of R = 1.1. EDS spectra showed that the composition of light gray phases is as same as that of matrix. The XRD pattern in Figure 3(a) also showed no crystal peak. Therefore, we presumed that the light gray phase is also a glassy phase which has similar composition with glassy matrix. It could be seen from Figure 5(a) that there precipitated many dendritic cuspidine crystals in the agitated sample, which is consistent with XRD results in Figure 5(a). This further verified the results that crystallization temperature of mold fluxes was increased with addition of agitation. As temperature gradually decreased, there precipitated some crystals with faceted morphology but still existed many small equiaxed dendrites in agitated samples. In comparison, most of crystals grew up with faceted morphology in static samples.

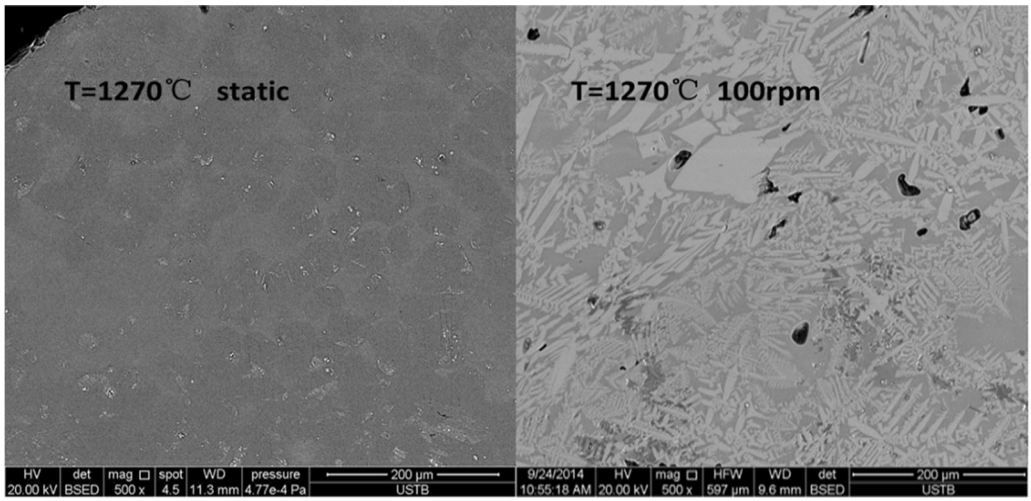

(a) T=1543K(1270°C)

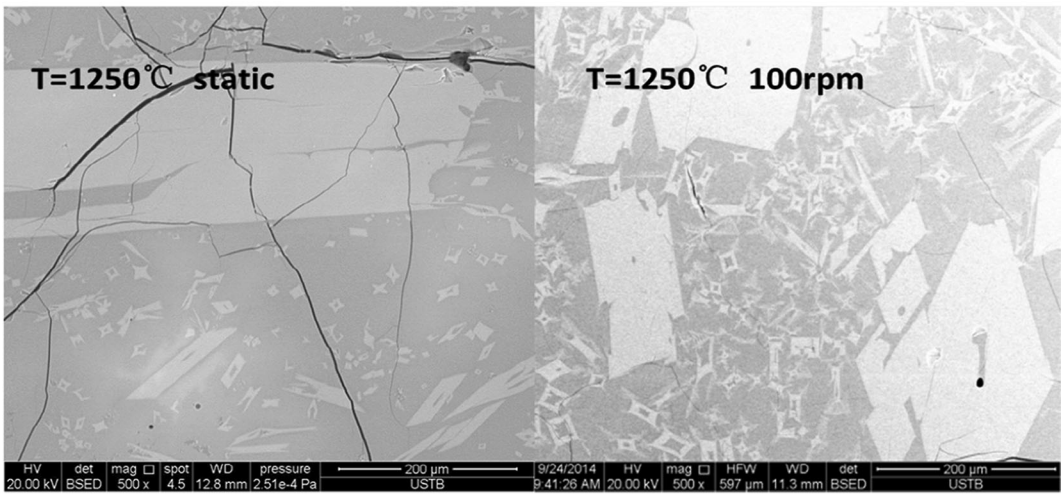

(b) T=1523K (1250°C)

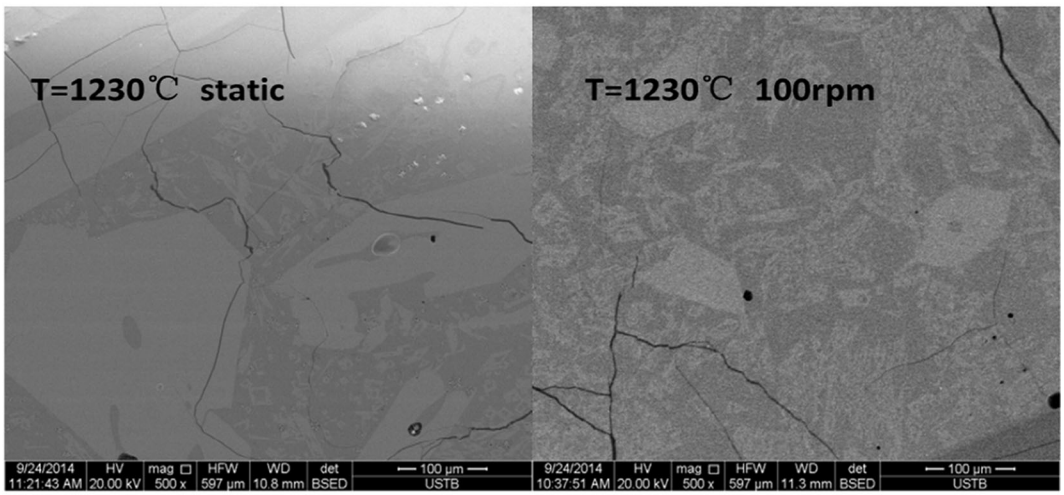

(c) T=1503K (1230°C)

Fig. 5—SEM images of the samples with a basicity of $R = 1.1$.

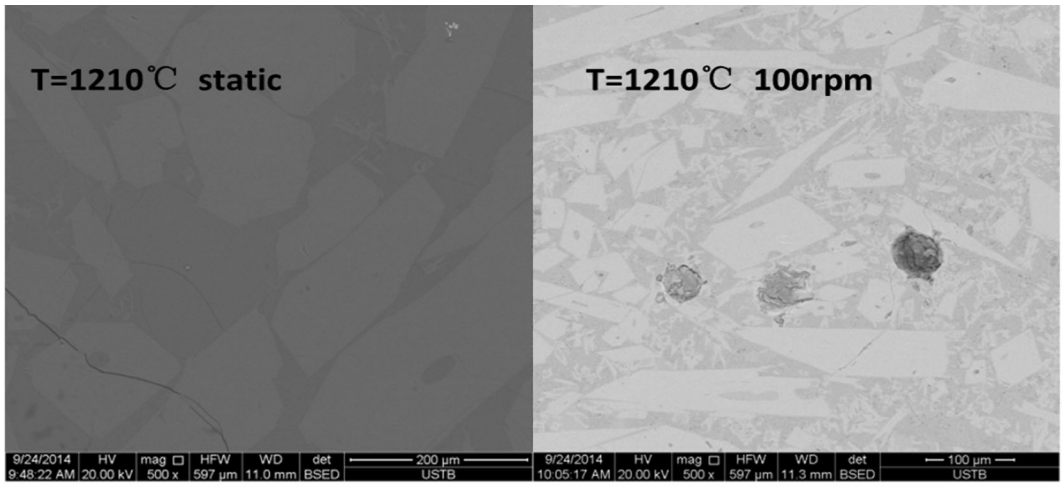

(d) T=1483K (1210°C)

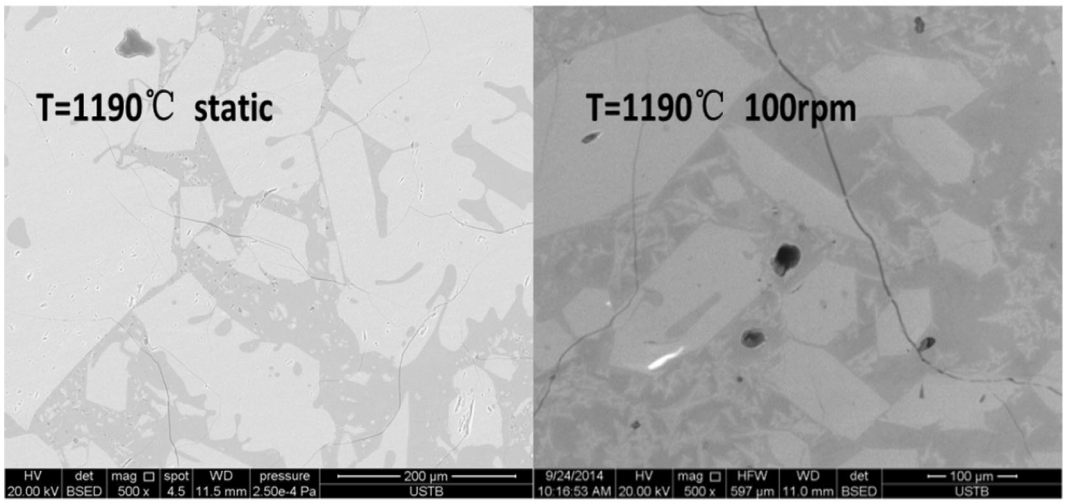

(e) T=1463K (1190°C)

Fig. 5—continued.

The agitation should have no influence on the thermodynamic of mold fluxes crystallization. It is found in Figures 3 and 5 that the crystallization product was not changed by agitation. The early crystallization of agitated sample could be due to enhanced heterogeneous nucleation of mold fluxes by agitation.[17] The flow of fluxes induced by rotation of Mo rod would accelerate the transportation across the liquid–crystal interface, and therefore enhances the nucleation rate of crystal. Besides, arms of dendrites precipitated at early stage of crystallization could be broken by agitation to form small fragments.[17,23] These small fragments could form heterogeneous nucleation sites and increase overall nucleation fraction. Therefore, heterogeneous nucleation could be enhanced by agitation of Mo rod. One could also consider some other possible nucleation sites. The Mo rod in melts and graphite could provide extra sites for heterogeneous nucleation. To check if there are some particles from oxidation of Mo in fluxes, the MoO_3 contents in fluxes were determined using XRF. The results showed that the content of MoO_3 is 0.09 and 1.09 pct for samples with $R = 1.1$ and 1.2, respectively. The lower content of MoO_3 in slag indicated that the oxidation of Mo in the present experiments is not very significant. Graphite crucible could also provide extra sources for heterogeneous nucleation. The carbon contents in mold fluxes were also determined to check if there are some carbon particles. It was found that carbon contents in slag are as low as 0.062 pct, 0.07 pct for flux with $R = 1.1$ and 1.2, respectively, indicating that there is negligible carbon particle in mold fluxes.

The effect of Mo rod on the temperature distribution of melts should be also discussed. The high thermal conductivity of Mo rod could lower the temperature and promote crystallization of melts near the rod during cooling. In the present experiment, 15-minutes isothermal stage could be helpful to homogenize the temperature of melts. There could be some effects of Mo rod on temperature distribution and crystallization of melts in the cooling stage. In isothermal stage, the effect of Mo

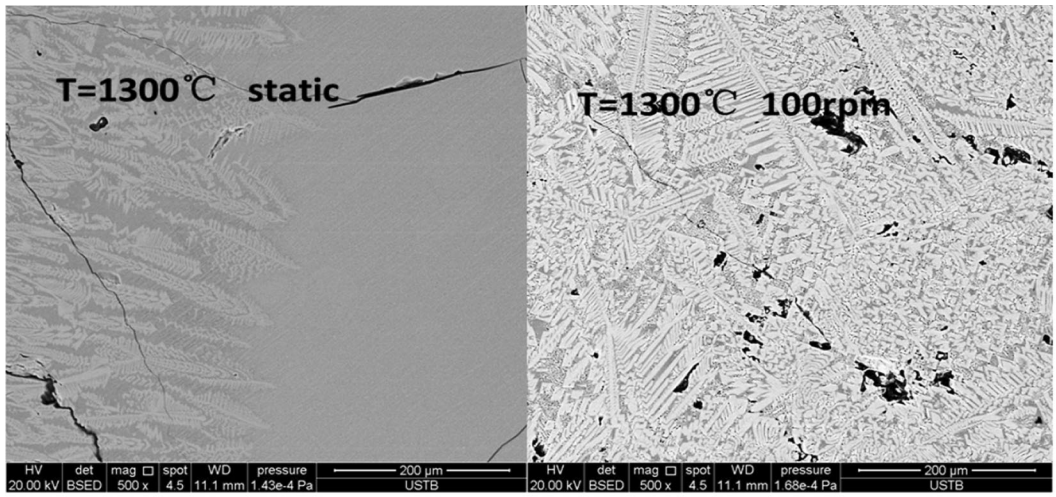

(a) T=1573K (1300°C)

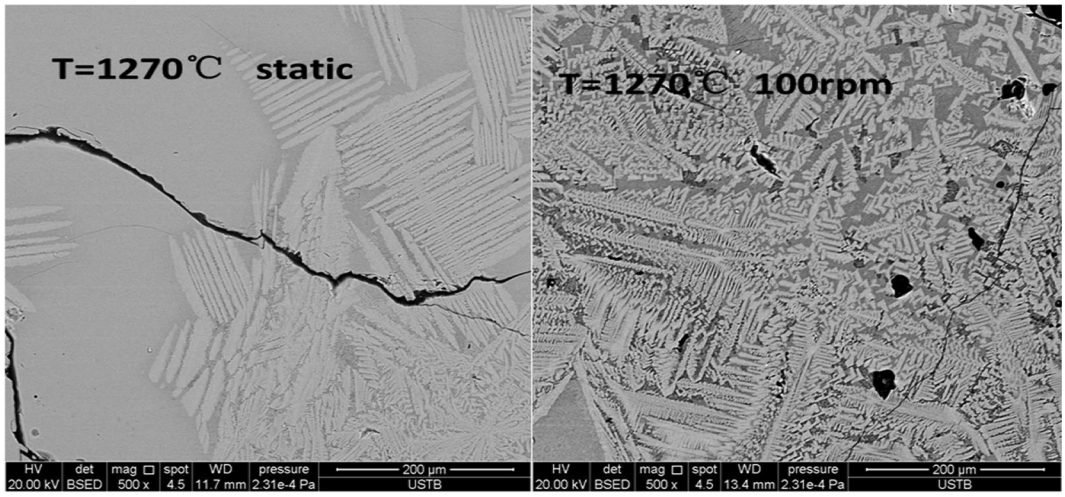

(b) T=1543K (1270°C)

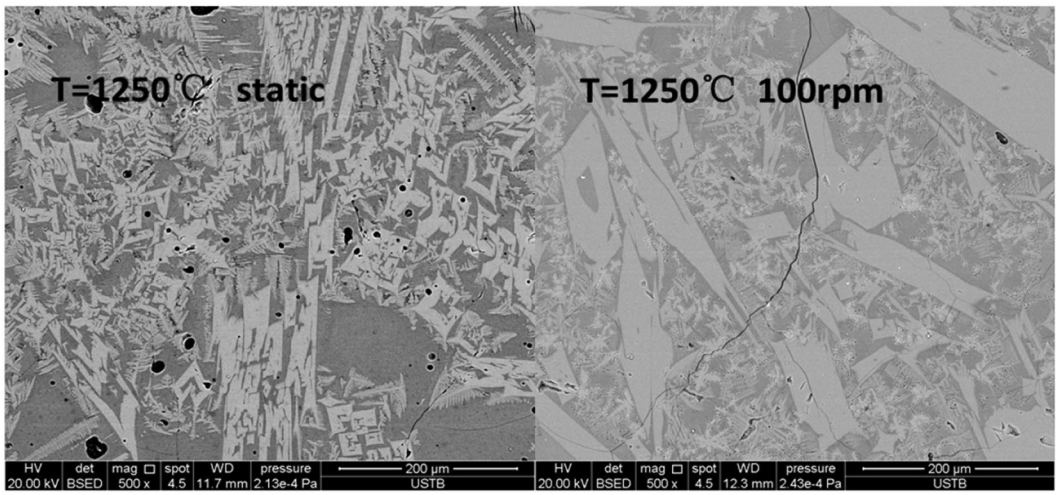

(c) T=1523K (1250°C)

Fig. 6—SEM images of the samples with a basicity of $R = 1.2$.

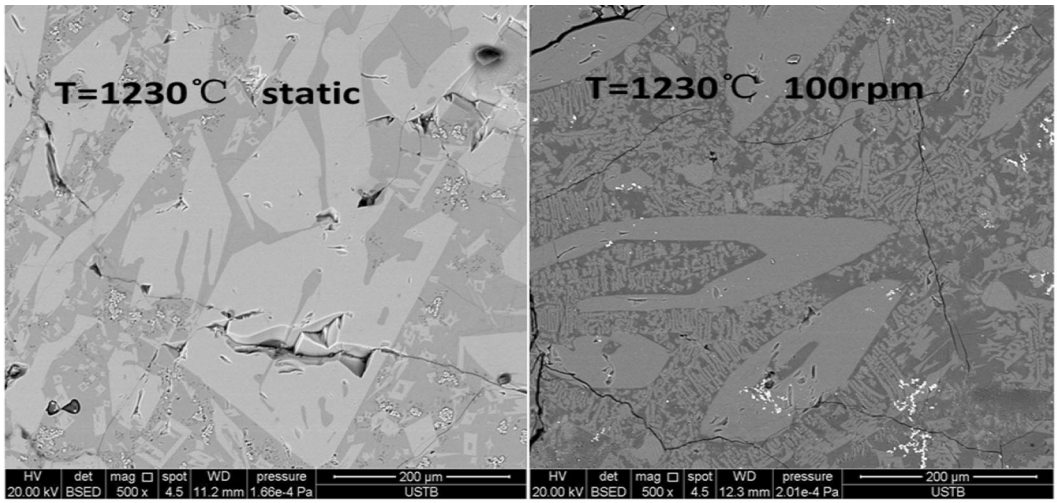

(d) T=1503K (1230°C)

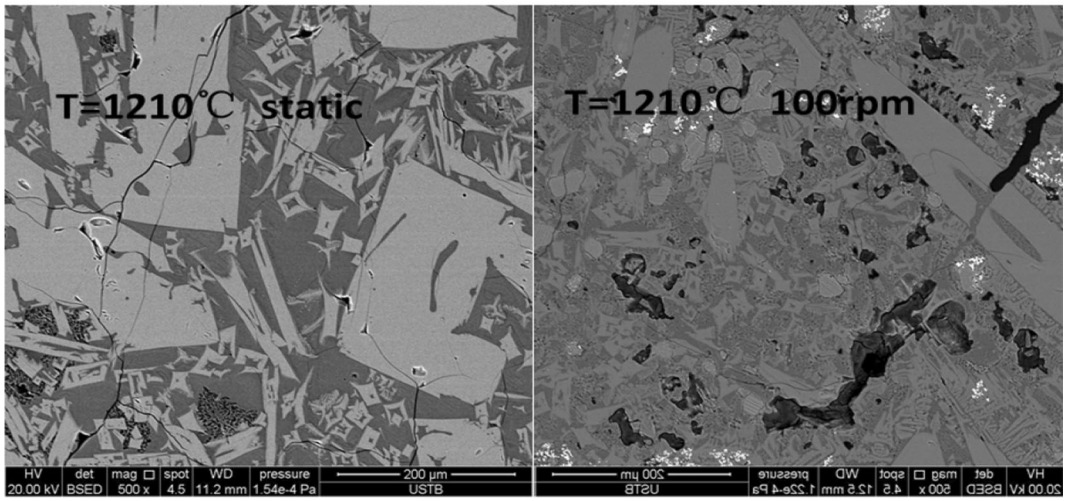

(e) T=1483K (1210°C)

Fig. 6—continued.

Table III. The Crystalline Fraction at Various Temperatures of the Investigated Mold Fluxes

	Crystalline Fraction (vol pct)					
Sample	1573 K (1300 °C)	1543 K (1270 °C)	1523 K (1250 °C)	1503 K (1230 °C)	1483 K (1210 °C)	1463 K (1190 °C)
R = 1.1						
Static	—	0	50.3	60.6	67.9	75.6
Dynamic	—	58.9	60.1	69.9	74.4	75.1
R = 1.2						
Static	10	20.7	51.5	59.1	68.8	—
Dynamic	60.9	70.1	73.9	75.6	76.9	—

rod on temperature and crystallization could gradually become negligible.

Figure 6 shows micrographs of samples with R = 1.2 quenched at different temperatures. Directional growth of dendrites from left to right side could be found in the static sample quenched at 1573 K (1300 °C), while a lot of dendrites with different orientations could be found in agitated sample quenched at 1573 K (1300 °C). The rotational flow of molten fluxes induced by agitation could lead to non-uniform orientations of dendrites. Some small equiaxed dendrites, which were formed by additional heterogeneous nucleation due to breakup and

fragmentation of the columnar dendrites caused by flow due to agitation, were also found in agitated sample.[23–25] Crystallization behaviors of samples with $R = 1.2$ at lower temperature are similar to those of samples with $R = 1.1$. The decrease of temperature also leads to growth of crystals with faceted morphology in samples with $R = 1.2$. There are still a lot of cuspidine dendrites in agitated samples with $R = 1.2$, and only a few cuspidine dendrites could be found in static samples.

It could be inferred from above observation that agitation field was conducive to the formation of small dendritic cuspidine. The fact that dendritic cuspidine tends to be formed in agitated samples may be due to several reasons. The enhanced heterogeneous nucleation of crystal by agitation of Mo rod could lead to formation of small crystal nucleus which would grow up to be small dendrites. The agitation could accelerate the flow of melts in crucible and lead to more uniform temperature distribution. Transportation of latent heat toward solidification front most likely induces a fragmentation of columnar dendrites due to thermal remelting.[23–25] Therefore, a numerous increase of dendritic fragments could be observed ahead of the solidification front. It could be also observed that the sizes of faceted crystals in agitated samples are smaller than those in static samples. The precipitation of numerous small dendrites would lead to smaller undercooling of remaining molten fluxes. Since growth of faceted crystal is controlled by interfacial reaction, the decreased undercooling would have stronger influence on crystal growth of faceted growth than increased heat and mass transfer.[22] Accordingly, the growth of faceted crystals was slightly suppressed by agitation.

Crystalline fraction could be estimated by measuring the areas of glassy matrixes and crystals using the software of Image-Pro Plus, and listed in Table III. It can be found that the crystallization fraction of agitated samples is much larger than static samples in the initial stage of crystallization. As temperature was further decreased, the influence of agitation on crystalline fraction of sample becomes smaller. The heterogeneous nucleation was significantly enhanced by agitation in the initial stage of crystallization, leading to much higher crystalline fractions of quenched samples. At lower temperature, the formation of small dendrites was induced by agitation, but the growth of faceted crystal was suppressed by agitation. Therefore, the overall crystalline fraction of agitated sample is only slightly larger than that of static sample.

IV. CONCLUSIONS

The effect of agitation on the crystallization behavior of $CaO\text{-}Al_2O_3\text{-}SiO_2\text{-}Na_2O\text{-}CaF_2$ mold fluxes was investigated by stirring molten fluxes with rotating Mo rods. Following conclusions could be drawn:

1. Crystallization temperatures of samples under the agitation were higher than those of samples in static condition.
2. The agitation field was conducive to the formation of small cuspidine dendrites. Meanwhile, the agitation field could decrease the size of faceted crystal.
3. Crystalline fraction of sample under agitation is much larger than those of sample in static condition in the initial stage of crystallization. The effect of agitation on crystalline fraction becomes much weaker at lower temperature.

ACKNOWLEDGMENTS

Financial supports from the Natural Science Foundation of China (NSFC Contract Nos. 51174018, 51174022) and Fundamental Research Funds for the Central Universities (FRF-TP-14-108A2) are gratefully acknowledged.

REFERENCES

1. C. Pinheiro: *Iron Steelmaker*, 1995, vol. 22, pp. 43–44.
2. K.C. Mills and A.B. Fox: *ISIJ Int*., 2003, vol. 10, pp. 1479–86.
3. K.C. Mills, A.B. Fox, Z. Li, and R.P. Thackray: *Ironmak. Steelmak*., 2005, vol. 1, pp. 26–34.
4. K.C. Mills and A.B. Fox: *High Temp. Mater. Process*., 2003, vols. 5–6, pp. 291–302.
5. M. Persson, M. Görnerup, and S. Seetharaman: *ISIJ Int*., 2007, vol. 47, pp. 1533–40.
6. A.W. Cramb: *ISIJ Int*., 2014, vol. 54, pp. 2665–57.
7. M. Suzuki, H. Mizukami, T. Kitagawa, K. Kawakami, S. Uchida, and Y. Komatsu: *ISIJ Int*., 1991, vol. 3, pp. 254–61.
8. H. Takeuchi, S. Matsumura, R. Hidaka, Y. Nagano, and Y. Suzuki: *Tetsu-to-Hagané*, 1983, vol. 2, pp. 248–53.
9. S. Sukenaga, K. Kusada, N. Saito, and K. Nakashima: *High Temp. Mater. Process*., 2012, vol. 31, pp. 459–63.
10. N. Saito, K. Kusada, S. Sukenaga, Y. Ohta, and K. Nakashima: *ISIJ Int*., 2012, vol. 12, pp. 2123–29.
11. Y. Harada, K. Kusada, S. Sukenaga, H. Yamamura, Y. Ueshima, T. Mizoguchi, N. Saito, and K. Nakashima: *ISIJ Int*., 2014, vol. 9, pp. 2071–76.
12. C. Shi, M. Seo, J. Cho, and S. Kim: *Metall. Mater. Trans. B*, 2014, vol. 45B, pp. 1081–97.
13. L.J. Zhou, W.L. Wang, F.J. Ma, J. Li, J. Wei, H. Matsuura, and F. Tsukihashi: *Metall. Mater. Trans. B*, 2012, vol. 43B, pp. 354–62.
14. M.D. Seo, C.B. Shi, J.W. Cho, and S.H. Kim: *Metall. Mater. Trans. B*, 2014, . DOI:10.1007/s11663-014-0091-2.
15. H. Masahito: *ISIJ Int*., 2013, vol. 53, pp. 648–54.
16. J.L. Li, Q.F. Shu, and K.C. Chou: *Metall. Mater. Trans. B*, 2014, vol. 45B, pp. 1593–99.
17. W. Kurz and D.J. Fisher: *Fundamentals of Solidification*, Trans Tech Publications, Dürnten, 1986, p. 34.
18. C. Orrling, A. Tilliander, Y. Kashiwaya, and A.W. Cramb: *Iron Steelmaker*, 2000, vol. 20, pp. 53–63.
19. C. Orrling, S. Sridhar, and A.W. Cramb: *High Temp. Mater. Process*., 2001, vol. 20, pp. 195–200.
20. N. Kölbl, I. Marschall, and H. Harmuth: *J. Mater. Sci*., 2011, vol. 46, p. 6248.
21. Q.F. Shu, Z. Wang, J.L. Klug, K.C. Chou, and P.R. Scheller: *Steel Res. Int*., 2013, vol. 84, pp. 1138–45.
22. RJ Kirkpatrick: *Am. Miner*., 1975, vol. 60, pp. 798–814.
23. C.M. Flemings: *Metall. Mater. Trans. B*, 1991, vol. 22B, pp. 269–93.
24. M.A. Martorano, C. Beckermann, and C.A. Gandin: *Metall. Mater. Trans. A*, 2003, vol. 34A, pp. 1657–74.
25. B.Willers, S. Eckert, U. Michel, I. Haase, and G. Zouhar: *Mater. Sci. Eng. A*, 2005, vol. 402, pp. 55–65.